Desalination and Water Treatment
www.deswater.com

doi: 10.5004/dwt.2018.21642

101 (2018) 31–36
January

Novel preparation of ceramic nanofiltration membrane for the removal of trace organic compounds

Youngkun Chung[a], Mi-Young Lee[a], Hosik Park[b], You-In Park[b], Seung-Eun Nam[b], Pyung Soo Lee[b], Yu Sik Hwang[c], Seoktae Kang[a,*]

[a]*Department of Civil and Environmental Engineering, Korea Advanced Institute of Science and Technology (KAIST), 291 Daehak-ro, Yuseong-gu, Daejeon 305-701, Korea, Tel. +82-42-350-3635; Fax: +82-42-350-3610; email: stkang@kaist.ac.kr (S. Kang)*
[b]*Center for Membranes, Advanced Materials Division, Korea Research Institute of Chemical Technology, 141 Gajeong-ro, Yuseong-gu, Daejeon 34114, Korea*
[c]*Future Environmental Research Center, Korea Institute of Toxicology, Jinju 660-844, Republic of Korea*

Received 27 August 2017; Accepted 28 October 2017

ABSTRACT

In this research, ceramic ultrafiltration (UF) membrane was modified to nanofiltration (NF) membrane by simple and novel filtration coating with approximately 45 nm of alumina–zirconia (Al–Zr) nanoparticles. The prepared ceramic NF membrane showed excellent performance with 15 LMH/bar of specific water flux, ~1,000 Da of molecular weight cut-off, and 58% of $CaCl_2$ rejection. The removal efficiency of tested trace organic compounds (TrOCs) was ranged from 2.2% ± 0.3% (caffeine) and 65.0% ± 2.1% (geosmin) at pH 7.4, and the major removal mechanisms of the prepared ceramic NF membrane were the size exclusion and electrostatic adsorption originated from the thick cross-sectional layer of positively charged Al–Zr nanoparticles deposited on the pores of ceramic UF membranes. The novel coating method for preparing ceramic NF membrane is expected to be applicable for the commercial manufacturing processes to remove TrOCs.

Keywords: Ceramic nanofiltration membrane; Filtration coating; Geosmin; Trace organic compounds

1. Introduction

Currently, the contamination of water resources is of increasing concern by various trace organic compounds (TrOCs), including pharmaceuticals and personal care products, algal toxins (2-MIB and geosmin), and industrial chemicals. The occurrence of TrOCs in aquatic systems has been studied with negative effects such as short- and long-term toxicity found to occur in different species [1–3]. There are very few discharge guidelines and standards which regulate TrOCs [4]. Commonly used water treatment processes to remove TrOCs mainly rely on advanced oxidation processes, ozonation, and activated carbon adsorption. These methods, however, are not specifically designed to remove TrOCs considering their unique property [4], whereas membrane processes such as nanofiltration (NF) and reverse osmosis (RO) can offer an effective solution to control these compounds [5]. Specifically, NF membranes are now widely used as an advanced means of water treatment, especially considering their lower energy requirements compared with RO membranes [6]. NF membranes are generally classified into two major groups, polymeric and ceramic membranes, depending on their material properties.

Previous studies found that ceramic membranes outperformed the polymeric types with regard to their operating conditions. The advantages of ceramic membranes included superior chemical and thermal resistivity, enabling chemical or thermal regeneration and sterilization by strong chemical or high-temperature processes. Moreover, their high mechanical stability enables high pressure back-washing. Thus, despite their higher cost, ceramic membranes are more

* Corresponding author.

economically feasible if used in water treatment processes that include harsh conditions [7,8].

Although ceramic NF membranes exhibit superior levels of thermal, mechanical, and chemical resistivity compared with polymeric membranes [7], their use in advanced water treatment processes has remained limited due to difficulties related to controlling the pore size during the conversion from ultrafiltration (UF) to NF membrane by means of dip-coating, spray-coating, spin-coating, and sputter-coating methods [8–10]. As an example, dip-coating method has been most widely used and studied for the preparation of a thin film on ceramic UF membranes. This method designated the deposition of a wet liquid film by withdrawal of a substrate from a nanoparticle medium. However, the crack was formed due to surface tension during drying and calcination process [10]. Spray-coating could cover a relatively large surface area effectively within a short preparation time. The biggest problem is that the final product has irregular surface [11]. Spin-coating has been suggested as another strategy to modify the membrane surface; however, it can be applied in flat-type membrane only [12]. Lastly, sputter-coating can fabricate the thin-film on the membrane using plasma and vacuum chamber [13], thus, it is not suitable to apply in commercial manufacturing processes, because it is too complicated and expensive. Overall, one of the difficulties to apply ceramic NF membranes for advanced water treatment is the lack of simple and efficient coating methods to produce defect-free membrane surfaces.

The objectives of the present study are to prepare ceramic NF membranes by a simple and novel filtration coating method, which forms a selective nanoparticle layer inside a ceramic UF membrane, and then to apply the prepared ceramic NF membrane for the removal of TrOCs such as geosmin and micropollutants.

2. Materials and methods

2.1. Fabrication of ceramic NF membrane by filtration coating

2.1.1. Preparation of coating nanoparticles (alumina (Al)–zirconia (Zr))

To prepare inorganic Al–Zr nanoparticles, 0.5 M aluminum nitrate nonahydrate (CAS no. 7784-27-2), 0.01 M zirconium(IV) oxychloride octahydrate (CAS no. 13520-92-8), 0.5 wt% polyvinyl alcohol (CAS no. 9002-89-5), and deionized water were mixed in 15:15:1:69 of volume ratio in the pH of 2.4 at 70°C for 6 h. The size and morphology of the prepared nanoparticles were analyzed by dynamic light scattering (DLS; Zetasizer Nano ZS, Malvern Instruments, UK) and scanning electron microscopy-energy dispersive spectrometry (SEM-EDS; Magellan 400, FEI Co., USA).

2.1.2. Preparation of ceramic NF membrane by filtration coating

Tubular-type ceramic UF membranes were prepared from α-alumina oxide (Al_2O_3) by a slip-casting technique which started from an aqueous suspension of aluminum oxide powder. After shaping of the support material by isostatic pressing, oxidation was performed at 1,000°C for 3 h [14]. The prepared Al–Zr nanoparticles solution was made to penetrate into the pores of casted ceramic UF membranes via the application of 10 bar of transmembrane pressure (TMP). At the same time, a cross-flow velocity (CFV) of 15 cm/s was provided to prevent the formation of irregular cake layer on UF membrane surfaces. The membrane coating process continued until the monitored flux was stabilized at 2.7 ± 0.3 LMH (Fig. 1), then, the membrane was placed in a microwave to evaporate surface water for 3 h and dried in an oven at 700°C for 3 h for the calcination of Al–Zr nanoparticles. After completing the membrane coating process, prepared Al–Zr ceramic membranes were characterized by SEM-EDS and surface potential measurements (SurPASS™ 3 device, Anton Paar, Austria) for pore size distribution and surface potential, respectively.

2.2. Measurement of membrane properties

The performance of the ceramic UF membranes and prepared NF membranes were assessed using a closed-loop lab-scale system containing a tubular-type membrane module. The test membrane was placed inside of the membrane module with an effective membrane area of 4.17×10^{-4} m^2. The feed solution was contained in a stainless steel vessel which was pressurized to 10 bar by nitrogen gas (99.99% purity) and circulated at the CFV of 10 cm/s. The system was operated in a closed loop so that the pressure on the feed side was stable during the experiment. A digital pressure gauge was connected to measure the TMP between the feed and permeate sides during the operation, and the data were loaded into a computer in real time [15].

During the operation of the membrane system, the pure water flux was monitored at different TMP levels of 0.5, 1, 2, and 3 bar for the ceramic UF membrane and 3, 5, 8, and 10 bar for the prepared NF membrane. The membrane resistance (R_m) was calculated by Darcy's law (1):

$$J_0 = \frac{\Delta P}{\mu R_m} \tag{1}$$

where J_0 denotes the pure water flux, ΔP is the TMP, R_m represents the membrane resistance, and μ is the dynamic viscosity of water (1.002×10^{-3} kg/m/s at 23°C).

To measure molecular weight cut-off (MWCO) and divalent salt rejection of ceramic UF and NF membranes, initial water flux was set to 150 LMH during all experiments; hence, the UF and NF membrane systems were operated at TMPs of 0.5 and 10 bar, respectively. MWCO was determined by polyethylene glycols (PEGs) with molecular weights of 200,

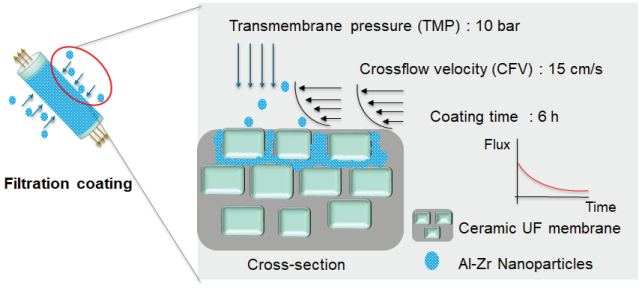

Fig. 1. A schematic diagram of the filtration coating method for the modification of the ceramic UF membrane.

400, 1,000, 2,000, and 6,000 Da. The concentrations of the feed were maintained to be 3 g/L, and the rejection was calculated by measuring total organic carbon (TOC) of feed and permeate stream using TOC analyzer (TOC-L, Shimadzu, Japan). Calcium chloride ($CaCl_2$) was used a model divalent salt at the feed concentration of 15 mM. The amount of salt rejection was calculated from the conductivity of feed and permeate. To confirm the reproducibility, all experiments were performed at least three times.

2.3. Rejection of TrOCs

The rejection of selected TrOCs was conducted to evaluate potential applicability of prepared ceramic NF membranes for advanced water treatment under operating conditions identical to those used in the salt rejection test. The characteristics of the TrOCs used in this study are shown in Table 1. TrOCs were purchased from Sigma-Aldrich (USA) and the experiments were tested at concentrations of 100 μg/L. The analysis was conducted on an HPLC-MS system (LC-MS 2020, Shimadzu, Japan) according to previous report [16].

During geosmin rejection test, the experiment was conducted at a geosmin (CAS no. 16423-19-1) concentration of 10 μg/L and at a pH of 7.4 ± 0.2. For extraction from the feed and permeate, amounts of 10 mL of the samples were collected in PTFE/silicone screw-cap amber glass vials. The fiber from solid-phase microextraction was inserted into the vial and exposed to the headspace above the aqueous sample for 30 min in a water bath at 70°C. After extraction, the fiber underwent gas chromatography–mass spectrometry (GC-MS; GC: 6890N, MS: 5973 Network, Agilent Technologies, USA) for thermal desorption and analysis. Helium was employed as a carrier gas at a constant column flow of 1 mL/min. The oven temperature started at 100°C and was held there for 5 min. It was then increased to 280°C at 20°C/min and held there for 19 min [17].

3. Results and discussions

3.1. Properties of prepared ceramic NF membrane

3.1.1. Properties of Al–Zr nanoparticles

The SEM image shown in Fig. 2 demonstrates the successful formation of Al–Zr nanoparticle gel with oxo bridges [18]. The DLS result shows that the average diameter of the nanoparticles was 44.42 ± 2.0 nm, which is smaller and more narrowly distributed than those of the single substances of the 0.5 M Al (334.1 ± 148.6 nm) and 0.01 M Zr nanoparticles (291.2 ± 66.8 nm) (Fig. 3). This may have been due to the hydrolysis and condensation of Al and Zr occurred under an acidic condition (pH 2.4) [18]. According to an EDS analysis conducted to determine the chemical properties of the nanoparticles, the element ratio of the prepared Al–Zr nanoparticles was composed with 87.5% of Al, 1.6% of Zr, and 10.9% of oxygen.

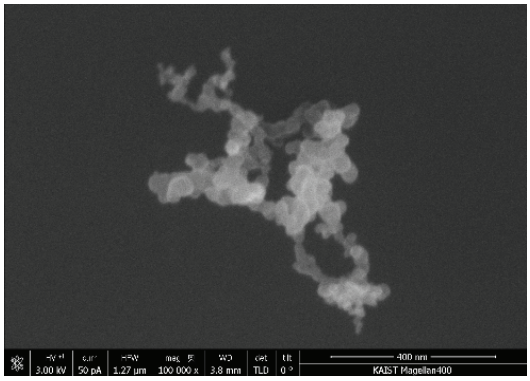

Fig. 2. A scanning electron microscopy (SEM) image of prepared Al–Zr nanoparticles.

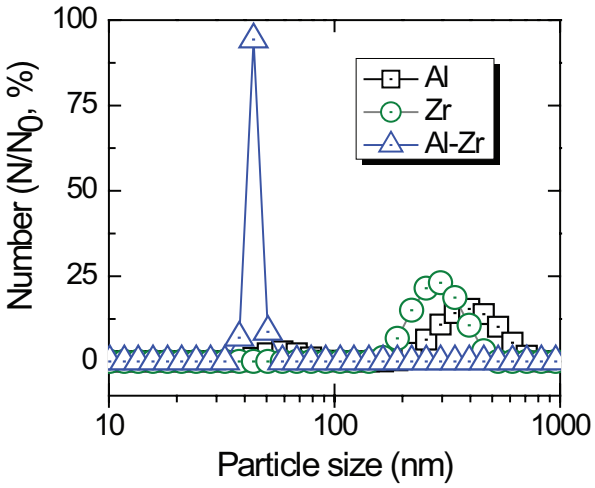

Fig. 3. Particle size distribution of nanoparticles measured by dynamic light scattering (DLS) (black square: 0.5 M alumina (Al) only, green circle: 0.01 M zirconia (Zr) only, and blue triangle: 0.5 M Al–0.01 M Zr, all of nanoparticles are dispersed in DI water containing 0.5 wt% of polyvinyl alcohol (PVA)).

Table 1
Physicochemical properties and removal efficiencies of selected trace organic compounds (TrOCs) by prepared ceramic NF membrane

Compounds	pK_a (net charge at pH 7.4)	Molecular weight (g/mol)	$\log K_{ow}$	Removal efficiency (%)
Geosmin	–0.01 (negatively charged)	183	3.70	65.0 ± 2.1
Acetaminophen	9.38 (neutral)	151	0.46	5.6 ± 2.8
Caffeine	14.00 (neutral)	194	–0.50	2.2 ± 0.3
Carbamazepine	13.94 (neutral)	236	2.45	4.3 ± 0.7
Linuron	11.94 (neutral)	249	3.20	22.7 ± 1.2
Triclosan	8.14 (neutral)	290	4.76	62.7 ± 2.1

3.1.2. Physicochemical properties of ceramic NF membrane

Fig. 4 shows SEM images of the ceramic UF and NF membranes. The pores with several hundred nanometers of the UF membrane were successfully covered with Al–Zr nanoparticles without cracks as shown in Figs. 4(a) and (b). Figs. 4(c) and (d) depict cross-sections of UF and NF membrane layers, indicating that Al–Zr nanoparticles were successfully filled pores of ceramic UF membrane to the thickness about 5 μm. In comparison with previous researches on the fabrication of ceramic NF membranes by a dip-coating and spray-coating method, the fabrication of NF was occurred during the deposition of Al–Zr nanoparticles. Thus, the active layer inside of the membrane surface is generated by penetrated Al–Zr nanoparticles with given 10 bar of TMP during filtration coating process (Fig. 4(d)). Moreover, the smooth membrane surface could be obtained with combination of high CFV (15 cm/s).

Fig. 5 shows the pore size distributions of UF and NF membranes. The average pore size of ceramic UF membrane was 303.2 ± 118.3 nm, while the pore size of the fabricated ceramic NF membrane was dramatically decreased to 4.3 ± 0.7 nm with significantly narrow distribution. It implied that fabricated NF membrane might provide good MWCO performances. Meanwhile, the surface charges of the membranes were not significantly different between the UF (6.0 ± 0.9 mV) and NF (10.6 ± 0.2 mV) membranes, indicating that the Al–Zr nanoparticles did not alter the zeta potential of the membrane (data not shown).

3.2. Membrane performance

3.2.1. Pure water flux

Fig. 6 shows the pure water fluxes of ceramic UF and NF membranes at different TMPs, with the slopes indicating the specific water flux. These results revealed that the water flux

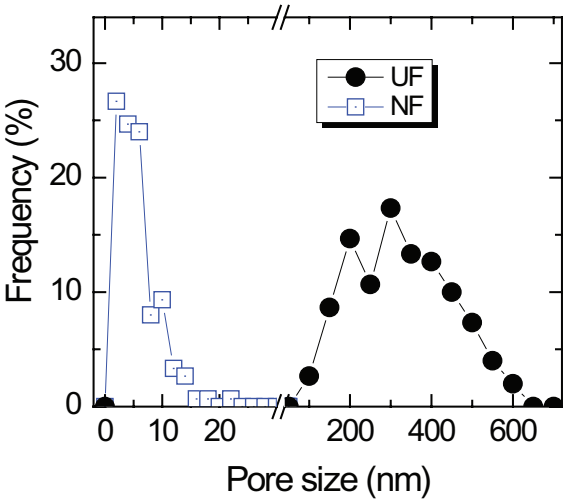

Fig. 5. Pore size distribution of ceramic UF and NF membranes ananlyzed by digital image processing of scanning electron microscopy (SEM).

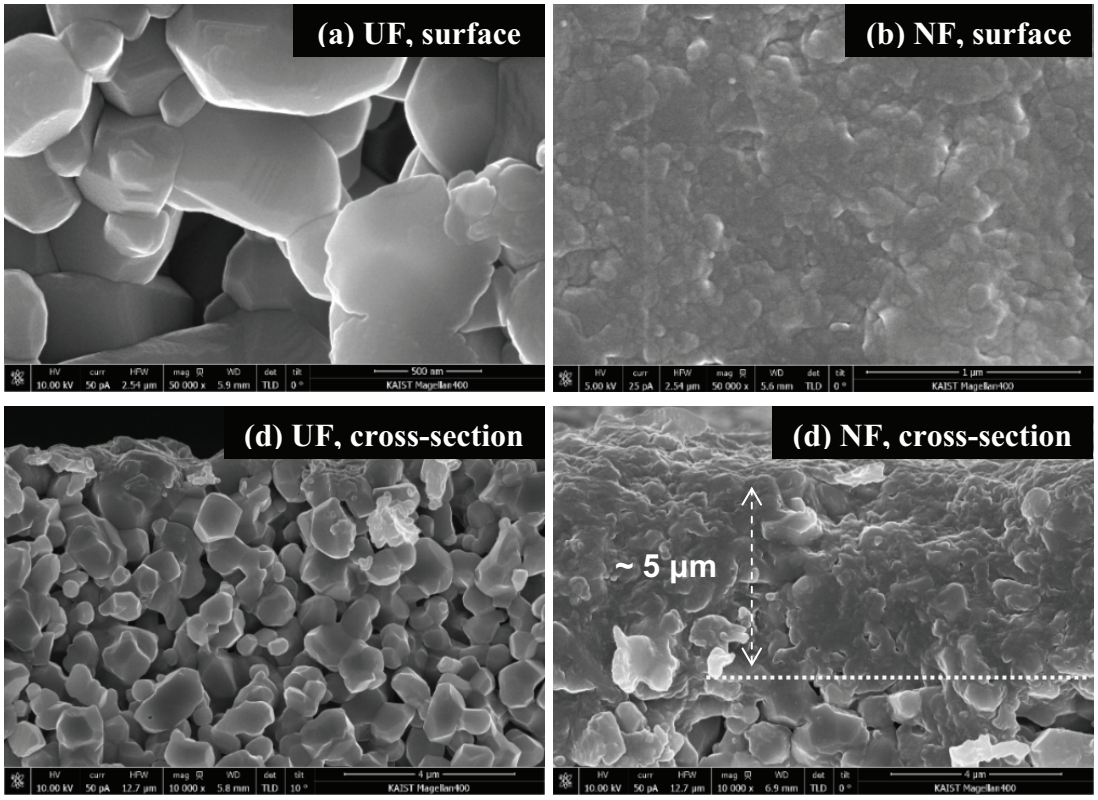

Fig. 4. Scanning electron microscopy (SEM): (a) and (c) surface and cross-section of ceramic UF membrane, (b) and (d) surface and cross-section of ceramic NF membrane.

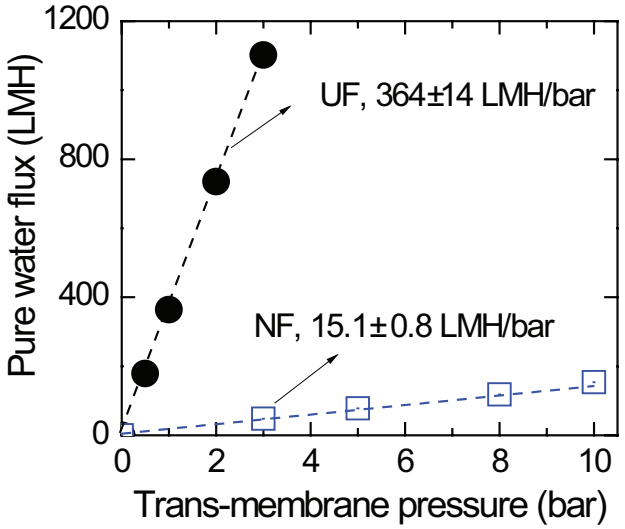

Fig. 6. Pure water fluxes of ceramic UF and NF membranes at different transmembrane pressure.

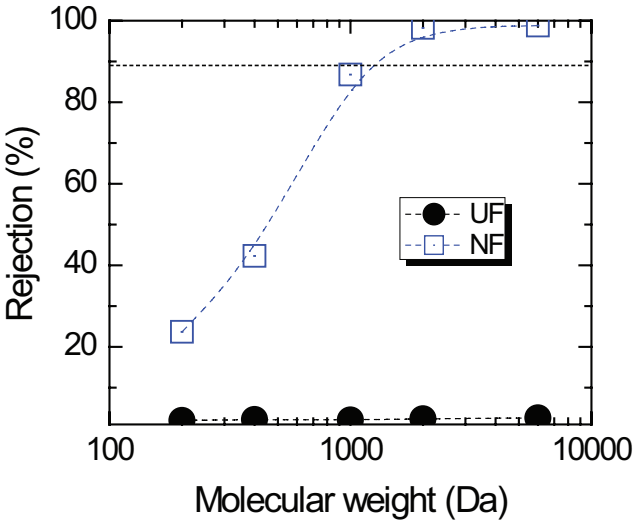

Fig. 7. Polyethylene glycol (PEG) rejection of ceramic UF and NF membranes. Experimental condition: pH of 7.4 ± 0.2, flux of 150 LMH, CFV of 10 cm/s, and temperature of 23°C ± 1°C.

of prepared ceramic NF membrane (15.1 ± 0.8 LMH/bar) was much lower than that of UF membrane (364 ± 14 LMH/bar) as expected. The membrane resistance (R_m) was calculated based on the results of the specific flux, and the resistance (2.38×10^{13}/m) of the fabricated NF membrane was within the typical resistance range of NF membranes (10^{12}–10^{13}/m). Therefore, above observations offer that the filtration coating of ceramic UF membrane using Al–Zr nanoparticles successfully fabricated ceramic NF membranes by plugging macropores of UF membrane, and creating nanopores through the deposition of Al–Zr nanoparticles.

3.2.2. MWCO and divalent salt rejection

The rejection of PEG with various molecular weights for both ceramic UF and NF membranes are plotted in Fig. 7. It clearly showed that the PEG rejection of fabricated NF membrane was sharply increased around 500 Da, and in particular, when the molecular weight exceeded 1,000 Da, the PEG rejection was reached higher than 90%, which could be regarded 1,000 Da as MWCO of fabricated NF membrane. Meanwhile, the PEG rejection of ceramic UF membrane was below 5% in all ranges of molecular weights tested here.

The performance of fabricated NF membrane was also evaluated through a rejection of divalent salts. Fig. 8 indicates that prepared NF membrane showed the remarkable increase in the removal of $CaCl_2$ (58.1% ± 0.9%) compared with ceramic UF membrane (4.2% ± 0.8%). As noted above, the pore size of NF membrane was successfully reduced to 4.3 nm by the novel coating method, as well as Al–Zr nanoparticles exhibited the positively charged membrane surface. Thus, both size exclusion and Donnan exclusion of Ca^{2+} might played significant role for the enhanced removal of divalent salts in the fabricated NF membrane.

3.3. Rejection of TrOCs

The removal efficiency of the Al–Zr ceramic NF membrane for various TrOCs is shown in Table 1. These results

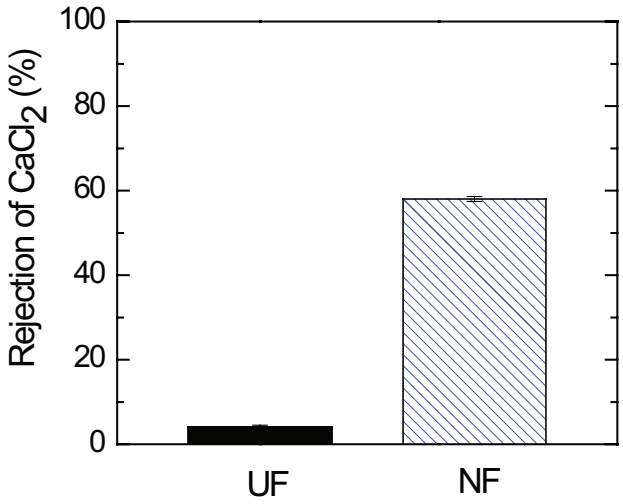

Fig. 8. The results of calcium chloride ($CaCl_2$) rejection of ceramic UF and NF membranes. Experimental condition: 15 mM of $CaCl_2$, pH of 7.4 ± 0.2, 10 cm/s of cross-flow velocity (CFV) in room temperature (23°C ± 1°C).

confirmed that TrOCs with higher molecular weights were more effectively removed in general: 5.6% ± 2.8% for acetaminophen (151 Da), 2.2% ± 0.3% for caffeine (194 Da), 4.3% ± 0.7% for carbamazepine (236 Da), 22.7% ± 1.2% for linuron (249 Da), and 62.7% ± 2.1% for triclosan (290 Da).

This outcome was in good agreement with the findings of previous research which reported that size exclusion was the major removal mechanism of micropollutants at neutral pH levels [19].

Interestingly, although all TrOCs except acetaminophen have higher molecular weights, geosmin exhibited the highest removal efficiency (65.0% ± 2.1%). This phenomenon could be explained by the charge effect, as discussed in relation to another mechanism in NF membranes. Electrostatic attraction occurred between the negatively charged geosmin

and the positively charged surface of the Al–Zr ceramic NF membrane in the neutral pH [20]. Consequently, the thick cross-sectional layer, which was formed by Al–Zr nanoparticles, resulted the adsorption of geosmin. This implies that the removal mechanism between the Al–Zr ceramic NF membrane and the TrOCs was not only size exclusion and but also the electrostatic adsorption in the case of charged pollutants such as geosmin.

4. Conclusions

We proposed a simple and novel coating method of ceramic UF membrane using Al–Zr nanoparticles and cross-flow filtration system. Al–Zr nanoparticles were successfully filled UF pores, and the fabricated membrane exhibited NF membrane performances in pure water flux, MWCO, and divalent salt rejection. Moreover, prepared NF membrane removed geosmin and TrOCs up to 65%, thus could be applied as an advanced water treatment process. Consequently, the filtration coating method can be applied for the fabrication of ceramic NF membranes in simple and reproducible conditions.

Acknowledgments

This subject is supported by Korea Ministry of Environment as "Global Top Project (2016002100008)" and by the Ministry of Trade, Industry and Energy (MOTIE), Korea Institute for Advancement of Technology (KIAT) through the Encouragement Program for The Industries of Economic Cooperation Region (R0004881).

Symbols

J_0 — Pure water flux
ΔP — Transmembrane pressure
R_m — Membrane resistance
μ — Dynamic viscosity of water

References

[1] S.D. Richardson, Disinfection by-products and other emerging contaminants in drinking water, TrAC, Trends Anal. Chem., 22 (2003) 666–684.
[2] R.P. Schwarzenbach, B.I. Escher, K. Fenner, T.B. Hofstetter, C.A. Johnson, U. Von Gunten, B. Wehrli, The challenge of micropollutants in aquatic systems, Science, 313 (2006) 1072–1077.
[3] Y. Wenbo, Z. Hongde, C. Nazim, Treatment of organic micropollutants in water and wastewater by UV-based processes: a literature review, Crit. Rev. Environ. Sci. Technol., 44 (2014) 1443–1476.
[4] Y. Luo, W. Guo, H.H. Ngo, L.D. Nghiem, F.I. Hai, J. Zhang, X.C. Wang, A review on the occurrence of micropollutants in the aquatic environment and their fate and removal during wastewater treatment, Sci. Total Environ., 473 (2014) 619–641.
[5] A.W. Mohammad, Y.H. Teow, W.L. Ang, Y.T. Chung, D.L. Oatley-Radcliffe, N. Hilal, Nanofiltration membranes review: recent advances and future prospects, Desalination, 356 (2015) 226–254.
[6] Y. Han, Z. Xu, C. Gao, Ultrathin graphene nanofiltration membrane for water purification, Adv. Funct. Mater., 23 (2013) 3693–3700.
[7] X. Zhang, T. Zhang, J. Ng, D.D. Sun, High-performance multifunctional TiO_2 nanowire ultrafiltration membrane with a hierarchical layer structure for water treatment, Adv. Funct. Mater., 19 (2009) 3731–3736.
[8] G. Mustafa, K. Wyns, P. Vandezande, A. Buekenhoudt, V. Meynen, Novel grafting method efficiently decreases irreversible fouling of ceramic nanofiltration membranes, J. Membr. Sci., 470 (2014) 369–377.
[9] J.W. Wang, L. Li, J.W. Zhang, X. Xu, C.S. Chen, β-Sialon ceramic hollow fiber membranes with high strength and low thermal conductivity for membrane distillation, J. Eur. Ceram. Soc., 36 (2016) 59–65.
[10] M.A. Aegerter, M. Mennig, Sol-Gel Technologies for Glass Producers and Users, Springer Science and Business Media, New York, 2004.
[11] L.B. Modesto-López, M. Miettinen, T. Torvela, A. Lähde, J. Jokiniemi, Direct deposition of graphene nanomaterial films on polymer-coated glass by ultrasonic spraying, Thin Solid Films, 578 (2015) 45–52.
[12] S. Hosaka, Updates in Advanced Lithography, InTech, Croatia, 2013.
[13] P. Huang, C. Huang, M. Lin, C. Chou, C. Hsu, C. Kuo, The effect of sputtering parameters on the film properties of molybdenum back contact for CIGS solar cells, Int. J. Photoenergy, 2013 (2013) 1–8.
[14] M.G. Ivanov, Y.L. Kopylov, V.B. Kravchenko, K.V. Lopukhin, V.V. Shemet, YAG and Y_2O_3 laser ceramics from nonagglomerated nanopowders, Inorg. Mater., 50 (2014) 951–959.
[15] P. Fagkaew, K. Ruengruehan, J. Chung, S. Kang, Relating intrinsic membrane water permeability and fouling propensity in forward osmosis processes, Desal. Wat. Treat., 77 (2017) 122–128.
[16] M. Xie, W.E. Price, L.D. Nghiem, M. Elimelech, Effects of feed and draw solution temperature and transmembrane temperature difference on the rejection of trace organic contaminants by forward osmosis, J. Membr. Sci., 438 (2013) 57–64.
[17] C. Martínez, N. Ramírez, V. Gómez, E. Pocurull, F. Borrull, Simultaneous determination of 76 micropollutants in water samples by headspace solid phase microextraction and gas chromatography–mass spectrometry, Talanta, 116 (2013) 937–945.
[18] W. Zhang, F.P. Glasser, Condensation and gelation of inorganic ZrO_2-Al_2O_3 sols, J. Mater. Sci., 28 (1993) 1129–1135.
[19] J. Radjenović, M. Petrović, F. Venturac, D. Barcelo, Rejection of pharmaceuticals in nanofiltration and reverse osmosis membrane drinking water treatment, Water Res., 42 (2008) 3601–3610.
[20] R. Chen, Q. Xue, Z. Zhang, N. Sugiura, Y. Yang, M. Li, Z. Lei, Development of long-life-cycle tablet ceramic adsorbent for geosmin removal from water solution, Appl. Surf. Sci., 257 (2011) 2091–2096.